

## A simple and accurate method for detecting cube corner rotations<sup>\*</sup>

Mikhail N. Matveev<sup>\*</sup>

<sup>\*</sup> *Moscow Institute of Physics and Technology, Institutskii per. 9,  
Dolgoprudny 141700 Russia (e-mail: miklem@mail.mipt.ru).*

---

**Abstract:** Cube corners are used widely in position detecting devices. A cube corner is attached to an object of interest. Then the position of the object is determined as the distance and two angles of direction to the cube corner. Recent developments make it possible to use a cube corner to detect the orientation of an object as well. However orientation cannot be measured directly, instead it should be recovered from other data. The paper introduces a method of calculating the orientation of a cube corner and shows that the method has an accuracy restricted by the accuracy of direct measurements only. Hence it detects orientation angles of a cube corner up to arc seconds.

*Keywords:* High accuracy pointing; Guidance, navigation and control of vehicles; Trajectory tracking and path following

---

### 1. INTRODUCTION

Cube corners return any light ray hitting them in exactly the opposite direction. This feature makes cube corners used widely in position detecting devices. A cube corner is attached to an object of interest. Then the position of a cube corner is determined as the distance to the cube corner and two angles of direction. Recent developments allow determining not only the position but also the orientation of a cube corner.

Provided a sufficient accuracy, applications of determining orientation are rich and welcome. It suffices to mention measuring hidden objects, controlling manipulations of robots, directing spacecrafts towards docks and so on. One of the problems bounding these applications is that the parameters determining the position of an object are measured directly, while the parameters determining the orientation of an object need to be calculated from other data.

To do this calculation, one should choose a set of parameters (angles) that will describe the orientation of an object, then develop another set of parameters (measured data) that depend on the parameters in the first set and can be measured directly, and finally find a numerical method that will recover the parameters in the first set from the parameters in the second. The method should be simple enough to admit unmanned usage and have a good accuracy.

The paper concerns two approaches to detecting orientation. One approach can be found in Bridges et al. (2010). It is based on viewing an image of the cube corner edges near the apex obtained by the projection along the optical axis. The other approach is initiated in Matveev (2014). It again uses the projection along the optical axis but analyzes an image of the entire light flow returned by the cube

corner. We present a method of calculating orientation angles developed for the second approach and show that the method is simple, accurate and fast enough.

### 2. ORIENTATION VIA AN IMAGE OF THE CUBE CORNER EDGES NEAR THE APEX

Bridges et al. (2010) describes the orientation of a cube corner by three angles of rotation about the three axes of a coordinate system defined as in Figure 1. The  $x$  axis of the coordinate system is chosen along the outer normal to the cube corner entrance facet. The three reflecting surfaces of the cube corner meet each other in three lines of intersection. The  $xy$  plane is defined as passing through the  $x$  axis and one of the intersection lines. The  $xy$  plane contains the  $y$  axis, which is perpendicular to the  $x$  axis. The  $z$  axis is perpendicular to both  $x$  and  $y$  axes.

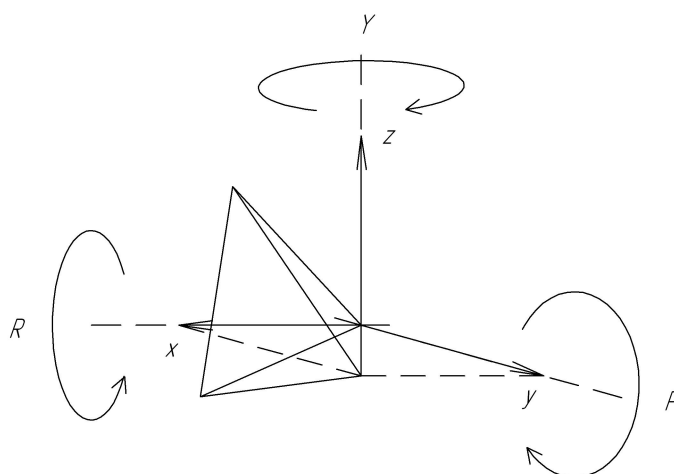


Fig. 1. A coordinate system to use with  $P$ ,  $Y$ , and  $R$  angles of orientation

---

<sup>\*</sup> Devoted to Ann.

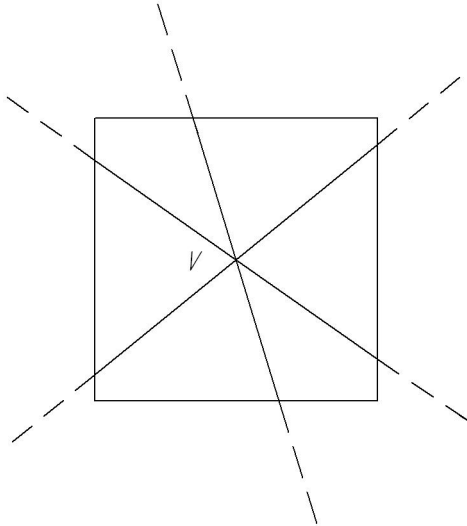


Fig. 2. An image of the edges of a cube corner

The cube corner is first rotated about the  $y$  axis by the pitch angle  $P$ . As a result of this rotation the coordinate system  $zyz$  becomes a coordinate system  $x'y'z'$  with  $y' = y$ . Then the cube corner is rotated about the  $z'$  axis by the yaw angle  $Y$ . As a result of this rotation the coordinate system  $x'y'z'$  becomes a coordinate system  $x''y''z''$  with  $z'' = z'$ . Finally, the cube corner retro reflector is rotated about the  $x''$  axis by the roll angle  $R$ . The angles  $P$ ,  $Y$ , and  $R$  determine the orientation of the cube corner.

To calculate the angles of rotation, Bridges et al. (2010) uses an orientation camera capturing the image of light intensities in the vicinity of the apex of the cube corner. As the reflecting surfaces scatter light where they meet each other, the image consist of three dark lines and looks like Figure 2. The dark lines are images of the edges of the cube corner and the point  $V$  is an image of the apex of the cube corner. Slopes  $m_1$ ,  $m_2$ , and  $m_3$  of the dark lines are measured to obtain the angles  $P$ ,  $Y$ , and  $R$  by solving the following system of equations

$$\begin{aligned}
 m_1 &= \frac{\sin P \cos Y / \sqrt{2} - \sin P \sin Y \cos R + \cos P \sin R}{\sin Y / \sqrt{2} + \cos Y \cos R} \\
 m_2 &= \frac{\sin P \cos Y / \sqrt{2} - \sin P \sin Y \cos(R + 120^\circ) + \cos P \sin(R + 120^\circ)}{\sin Y / \sqrt{2} + \cos Y \cos(R + 120^\circ)} + \\
 &\quad + \frac{\sin Y / \sqrt{2} + \cos Y \cos(R + 120^\circ)}{\cos P \sin(R + 120^\circ)} \\
 m_3 &= \frac{\sin P \cos Y / \sqrt{2} - \sin P \sin Y \cos(R + 240^\circ) + \cos P \sin(R + 240^\circ)}{\sin Y / \sqrt{2} + \cos Y \cos(R + 240^\circ)} + \\
 &\quad + \frac{\sin Y / \sqrt{2} + \cos Y \cos(R + 240^\circ)}{\cos P \sin(R + 240^\circ)}.
 \end{aligned} \tag{1}$$

A problem associated with system (1) is that it is essentially a system of three variables. The matter is that to make determining orientation an industrial application, one needs a method of numerical solution of system (1) that converges and provides an approximate solution of high accuracy. But how to find such a method? Attempts to solve system (1) by a numerical method in Matlab fail, and due to system (1) has three variables it is hard for a human even to realize (visualize) why it happens.

As a result another approach to determining the orientation of a cube corner is proposed in this paper. It is based on Matveev (2014), which advises to determine the orientation of an object not by an image of three lines in the vicinity of the apex of a cube corner but by an image of the entire light flow returned by a cube corner. By default the proposed approach recovers the dark lines discussed earlier, but also admits other orientation detecting opportunities. Below in this paper we explore in detail a realization of these opportunities that turns out especially useful as a computation technique.

### 3. ORIENTATION VIA AN IMAGE OF THE ENTIRE LIGHT FLOW RETURNED BY A CUBE CORNER

Let us realize what is the light flow returned by a cube corner. We will analyze the form of this flow in the plane of the entrance facet. Consider the (hypothetical) light ray hitting exactly the apex of the cube corner and reflecting in exactly the opposite direction. If the cube corner is not rotated, this ray gets in and out the entrance facet in its center of symmetry  $A$  (see Figure 3). In this case the intersection of the returned light flow and the entrance facet is the regular hexagon obtained by the intersection of the entrance facet with itself rotated by  $180^\circ$

The form of the returned light in the plane of the entrance facet of a rotated cube corner is found by a similar way. If the cube corner is rotated, the point where the ray hitting the apex gets in and out the entrance facet moves from its center of symmetry  $A$  to some other point  $B$ . Respectively, the form of the returned light flow through the entrance facet will become the intersection of the entrance facet with the itself rotated by  $180^\circ$  and shifted so that its center of symmetry moves to the point  $A'$  symmetric to the point  $A$  with respect to  $B$ , see Figure 3.

It is easy to see that the form of the light returned by a cube corner in the plane of its entrance facet is defined by two angles (see Figure 4). The angle  $\theta$  defines how much the normal to the entrance facet of the cube corner is deviated from its initial position. In other words, the angle  $\theta$  is the angle between the initial and deviated normals to

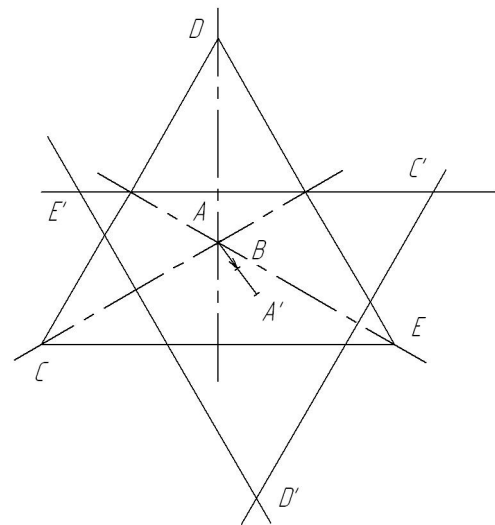


Fig. 3. Building the form of the light flow in the plane of the entrance facet of a cube corner

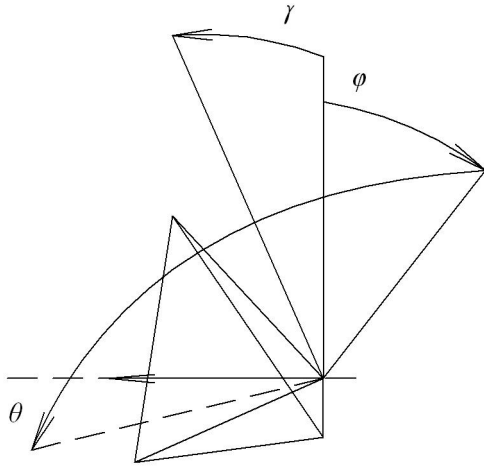


Fig. 4. A scheme of defining the angles of orientation  $\phi$ ,  $\theta$ , and  $\gamma$

the entrance facet. The other angle  $\phi$  defines in which side the normal is deviated from its initial position. Note that the angle  $\phi$  varies from 0 to 360°.

One more angle should be added to the angles  $\theta$  and  $\phi$  to complete the definition of orientation. We denote this extra angle by  $\gamma$  and assume that  $\gamma$  determines the rotation of the cube corner about the direction given by the normal to the entrance facet. We also assume that the rotation happens before the normal is deviated. Note that this choice of  $\gamma$  is in fact motivated by the constructions done in Figure 3, because building the form of the returned light, the angle  $\gamma$  defined as above influences only the angle  $\phi$  which becomes the angle  $\phi + \gamma$ .

To obtain an image of the light flow in the plane of the photosensitive array it suffices to project the form of the light flow in the plane of the entrance facet along the optical axis. Given the image, it is, of course, still possible to proceed exactly as in Bridges et al. (2010). One just needs to divide all edges of the image into two groups, the edges in any group not having common points. After that finding the intersection points of the lines given by the edges in each group (points  $C, D, E$ , and  $C', D', E'$  in Figure 3) leads to a pattern of three lines (lines  $CC', DD',$  and  $EE'$  in Figure 3) similar to the one shown in Figure 2. Respectively, a similar pattern brings similar problems.

So the next thing to do is to think of what to measure in the polygon being the image of a cube corner. Below we propose a set of data to measure that accounts for the advantages of the orientation angles  $\phi$ ,  $\theta$ , and  $\gamma$  schematically defined by Figure 3. Namely, as we deal with the polygonal form of the light flow returned by a cube corner, it is rather natural to measure the distances from the center of gravity of the image to its edges  $x_p$  and  $y_p$ , and the angle  $\gamma_p$ , say, between the lower edge and the horizontal direction.

Let us obtain the dependence of the distances  $x_p$  and  $y_p$  on the angles  $\phi$ ,  $\theta$ , and  $\gamma$ . Consider Figure 5, which is again done in the plane of the entrance facet of a cube corner. The line segment  $r$  joins the the center of symmetry of the entrance facet  $A$  with the point  $B$  where the light ray hitting the apex of a cube corner meets the entrance

facet. We have  $r = l \tan \theta_n$  where  $l$  is the distance from the apex of the cube corner to the entrance facet and  $\theta_n = \arcsin(\sin \theta/n)$  with  $n$  being the refraction index of the cube corner. The distance  $x$  from the point  $B$  to the lower edge of the retro reflector is given by the equation  $x = d - r \cos(\phi + \gamma)$  where  $d = l/\sqrt{2}$ . Thus we find that  $x = d - l \cos(\phi + \gamma) \tan \theta_n$ .

Repeating the same for one of the other edges we have the following system of equations

$$\begin{aligned} x &= d - l \cos(\phi + \gamma) \tan \theta_n, \\ y &= d - l \cos(120^\circ - \phi - \gamma) \tan \theta_n. \end{aligned} \quad (2)$$

Now recall that equations (2) hold in the plane of the entrance edge, but we measure the distances  $x_p$  and  $y_p$  in the plane of the photosensitive array. Hence we have  $x_p = x p(\phi + \gamma, \theta)$  and  $y_p = y p(120^\circ - \phi - \gamma, \theta)$ , where the function

$$p(\phi, \theta) = \frac{\sqrt{\cos^2 \phi + \sin^2 \phi \cos^2 \theta}}{\sin \phi \cos \phi (\cos^2 \theta - 1)}$$

accounts for the projection along the optical axis.

As a result, we write

$$\begin{aligned} \frac{x_p}{y_p} &= \frac{d - l \cos(\phi + \gamma) \tan \theta_n}{d - l \cos(120^\circ - \phi - \gamma) \tan \theta_n}, \\ \frac{x_p}{y_p} &= \frac{p(\phi + \gamma, \theta)}{p(120^\circ - \phi - \gamma, \theta)} \end{aligned} \quad (3)$$

It is also easy to see that the angle  $\gamma_p$  between the lower edge of the image of the cube corner and the horizontal direction is expressed as

$$\gamma_p = \arctan(\tan(\phi + \gamma) \cos \theta) - \phi. \quad (4)$$

Equations (3) and (4) constitute the entire system that expresses the dependencies of the measured values  $x_p$ ,  $y_p$ , and  $\gamma_p$  on the angles  $\phi$ ,  $\theta$ , and  $\gamma$  determining the orientation of a cube corner. It is easy to see that the system of equations (3) and (4) essentially differs from

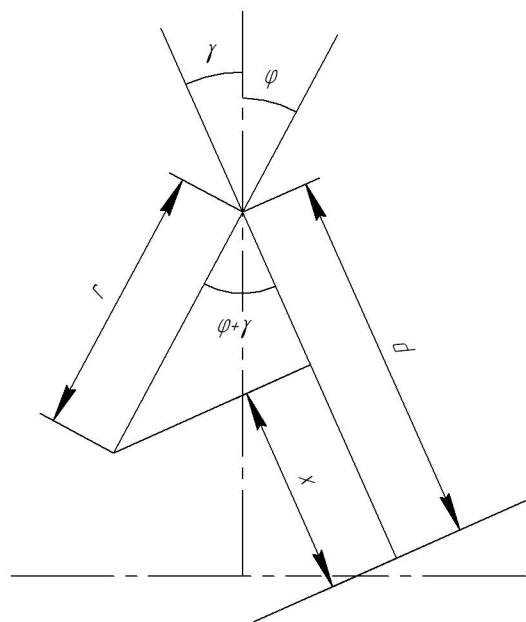


Fig. 5. The definition and computation of the distance  $x$

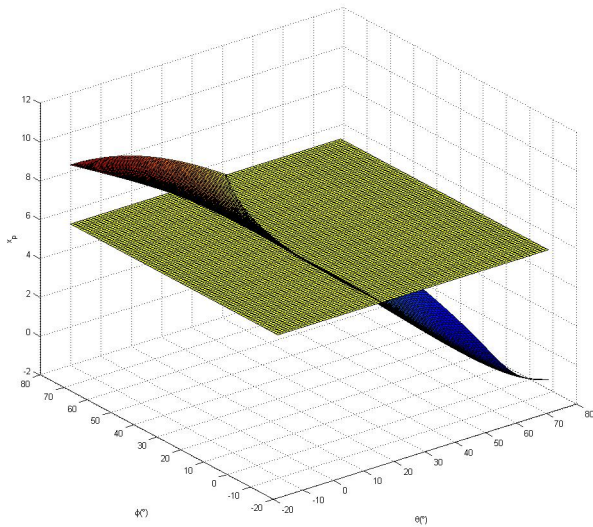


Fig. 6. A plot of the function  $X(\phi, \theta)$

system (1): introducing the angle  $\psi = \phi + \gamma$  reduces it to system (3) on the angles  $\psi$  and  $\theta$  and the separate formula

$$\gamma = \gamma_p + \psi - \arctan(\tan(\psi) \cos \theta). \quad (5)$$

expressing the dependence of the angle  $\gamma$  on the angles  $\psi$  and  $\theta$ .

Thus to determine the orientation of a cube corner it suffices now to solve system (3) of two variables. How difficult is to do it? To answer this question let us assume  $\gamma = 0$  to exclude  $\gamma$ ,  $\gamma_p$ ,  $\psi$ , and formulae (4),(5) from our consideration and introduce the function

$$X(\phi, \theta) = (d - l \cos \phi \tan \theta_n) p(\phi, \theta)$$

where  $l = 12.1$  and  $n = 1.51$ .

Then system (3) becomes the system

$$\begin{aligned} x_p &= X(\phi, \theta), \\ y_p &= X(120^\circ - \phi, \theta). \end{aligned} \quad (6)$$

Due to the symmetry of the entrance facet of a cube corner we may assume without loss of generality that the angle  $\phi$  varies from  $0^\circ$  to  $60^\circ$ . Another consideration allows us to limit the values of the angle  $\theta$ . As the light ray must pass the entrance facet, it is reasonable to think that the angle  $\theta$  also varies from  $0^\circ$  to  $60^\circ$ .

Now let us explore how the functions  $X(\phi, \theta)$  and  $X(120^\circ - \phi, \theta)$  look like. Figure 6 shows a plot of the function  $z = X(\phi, \theta)$  and the plane  $z = x_p = X(10^\circ, 20^\circ)$  in the slightly extended range  $-15^\circ \leq \phi \leq 75^\circ$  and  $-15^\circ \leq \theta \leq 75^\circ$ . It is easy to see that the set of points  $(\phi, \theta)$  where  $x_p = X(\phi, \theta)$  is an almost straight curve emanating along the line  $\theta = 20^\circ$ . Moreover we note that for every  $-15^\circ \leq \alpha \leq 75^\circ$  the line  $\phi = \alpha$  meets this curve only once and it follows from  $x_p = X(\alpha, \theta_\alpha)$  that  $x_p < X(\alpha, \theta)$  for all  $\theta < \theta_\alpha$  and  $x_p > X(\alpha, \theta)$  for all  $\theta > \theta_\alpha$ .

From these observations we find that to trace the curve  $x_p = X(\phi, \theta)$  in a region of interest it suffices to use the bisection method along lines  $\phi = \alpha$  with appropriate values of  $\alpha$  and the initial values of  $\theta$  being equal to  $-15^\circ$  and

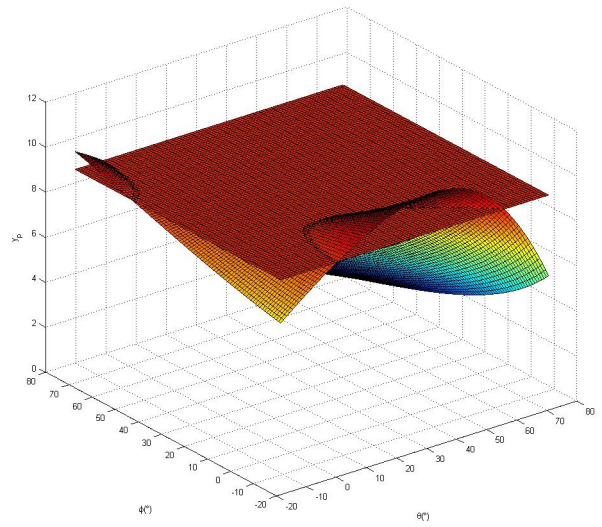


Fig. 7. A plot of the function  $X(120^\circ - \phi, \theta)$

$75^\circ$ . Now look at Figure 7 showing a plot of the function  $z = X(120^\circ - \phi, \theta)$  and the plane  $z = y_p = X(120^\circ - 10^\circ, 20^\circ) = X(110^\circ, 20^\circ)$  again in the range  $-15^\circ \leq \phi \leq 75^\circ$  and  $-15^\circ \leq \theta \leq 75^\circ$ .

We see that the curve  $y_p = X(120^\circ - \phi, \theta)$  in Figure 7 is of a bit more complex form, however this time we will be interested mainly of the signs of the values  $y_p - X(120^\circ - \phi, \theta)$  along the curve  $x_p = X(\phi, \theta)$ . To make things clearer both curves  $x_p = X(\phi, \theta)$  and  $y_p = X(120^\circ - \phi, \theta)$  are shown together in Figure 8. We find from Figures 7 and 8 that the curve  $x_p = X(\phi, \theta)$  meets the curve  $y_p = X(120^\circ - \phi, \theta)$  only once at the solution  $(\phi, \theta) = (10^\circ, 20^\circ)$  of system (6), for other points we have  $y_p < X(120^\circ - \phi, \theta)$  for all  $\phi < 10^\circ$  and  $y_p > X(120^\circ - \phi, \theta)$  for all  $\phi > 10^\circ$ .

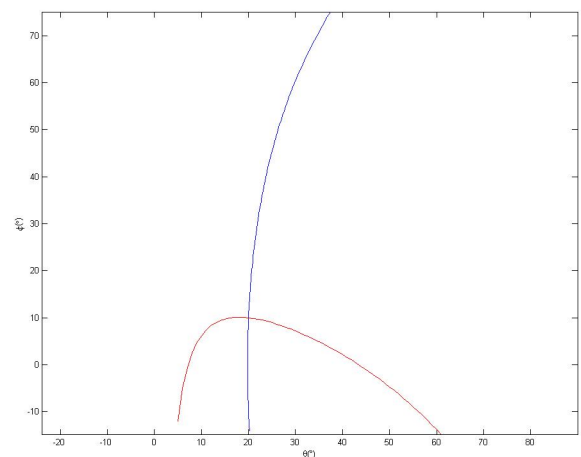


Fig. 8. A plot of the curves  $x_p = X(\phi, \theta)$  (blue) and  $y_p = X(120^\circ - \phi, \theta)$  (red)

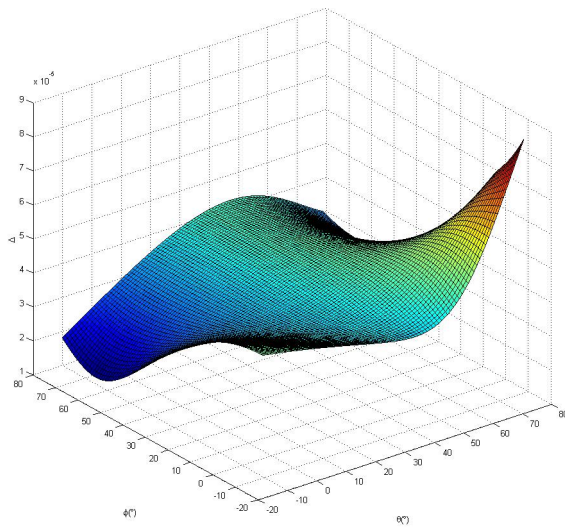


Fig. 9. A plot of the function  $\Delta(\phi, \theta)$

Thus we find that the solution  $(10^\circ, 20^\circ)$  again can be captured by applying the bisection method along the curve  $x_p = X(\phi, \theta)$  with the initial values of  $\phi$  being equal to  $-15^\circ$  and  $75^\circ$ . The appearance of the surfaces  $z = X(\phi, \theta)$  and  $z = X(120^\circ - \phi, \theta)$  in Figures 6 and 7 advises that the solution of system (6) can be archived in the same simple manner not only for  $x_p = X(10^\circ, 20^\circ)$  and  $y_p = X(110^\circ, 20^\circ)$  but also for all possible values  $x_p$  and  $y_p$ .

Let us try to give an estimation of the accuracy of the described above method of calculating the angles of orientation  $\phi$  and  $\theta$ . As the bisection methods gives any prescribed approximation, the accuracy of calculating  $\phi$  and  $\theta$  is, in fact, depend on, first, how do the distances  $x_p$  and  $y_p$  react on small changes of the angles  $\phi$  and  $\theta$  and, second, what is the accuracy of measuring  $x_p$  and  $y_p$  we are able to provide with the existing level of technology.

Consider the function

$$\Delta(\phi, \theta) = \sqrt{\Delta_x(\phi, \theta)^2 + \Delta_y(\phi, \theta)^2}$$

where

$$\begin{aligned} \Delta_x(\phi, \theta) &= X(\phi, \theta + 1'') - X(\phi, \theta), \\ \Delta_y(\phi, \theta) &= X(120^\circ - \phi, \theta + 1'') - X(120^\circ - \phi, \theta). \end{aligned}$$

The function  $\Delta(\phi, \theta)$  estimates the changes in the values of the distances  $x_p$  and  $y_p$  caused by the increase of one arc second in the value of  $\theta$ . A plot of the function  $\Delta(\phi, \theta)$  is shown on Figure 9.

It is easy to see that the mean value of  $\Delta(\phi, \theta)$  over the region  $0^\circ \leq \phi \leq 60^\circ$  and  $0^\circ \leq \theta \leq 60^\circ$  in Figure 9 is about  $5 \cdot 10^{-5}$ . Now recall that we use  $l = 12.1$  in the function  $X(\phi, \theta)$  what means that so is the distance from the apex of the cube corner to its entrance facet. It is natural to think that  $l$  is expressed in millimeters (mm), so the value  $5 \cdot 10^{-5}$  also means  $5 \cdot 10^{-5}$  mm.

Assuming that the pixel size of the photosensitive array is 0.02 mm and linear values are measured up to 0.03 of the pixel size, we conclude that we can register linear displacements up to  $0.03 \times 0.02$  mm =  $6 \cdot 10^{-4}$  mm, and,

hence, the angles of orientations  $\phi$  and  $\theta$  up to 10 arc seconds. This is an existing level of measurements. As the technology improves, the measurements up to one arc second do not seem to be unreachable.

Note that an estimation of the accuracy of calculating the angle  $\gamma$  is obtained in a similar way. Really, consider the function

$$\begin{aligned} \Delta_\gamma(\gamma) &= \arctan(\tan(10^\circ + \gamma + 1'') \cos 20^\circ) \\ &\quad - \arctan(\tan(10^\circ + \gamma) \cos 20^\circ) \end{aligned}$$

obtained from equation (4) and expressing the change in the value of  $\gamma_p$  caused by the increase of one arc second in the value of  $\gamma$  when  $\phi = 10^\circ$  and  $\theta = 20^\circ$ . A plot of the function  $\Delta_\gamma(\phi, \theta)$  is shown on Figure 10. It is clear from Figure 10 that to detect the change of one arc second in  $\gamma$  it is enough to register a change of a similar value in  $\gamma_p$ . Dukarevich and Dukarevich (2009) shows that this is possible already in the existing level of technology.

Finally let us estimate the cost of calculating  $\phi$  and  $\theta$ . The proposed method is essentially the double bisection first along lines  $\phi = \alpha$  and then along the curve  $x_p = X(\phi, \theta)$ . In both cases the initial range is about  $100^\circ$  (from  $-15^\circ$  to  $75^\circ$ ) and the final range is one arc second or  $1/3600^\circ$ . So the cost of calculating  $\phi$  and  $\theta$  up to one arc second by the proposed method is

$$(\log_2(100 \cdot 3600))^2 \approx 340$$

iterations, what is confirmed by test calculations.

#### 4. CONCLUSION

A cube corner is generally felt as small as a point, but, if one can measure its orientation, this point is a point with a coordinate system. The coordinate system is naturally given by the edges of the cube corner being the intersection of the reflecting facets. So, in fact, given a point, one knows also a coordinate system at this point and, hence, is also aware of the space around this point. Let us imagine what this knowledge brings.

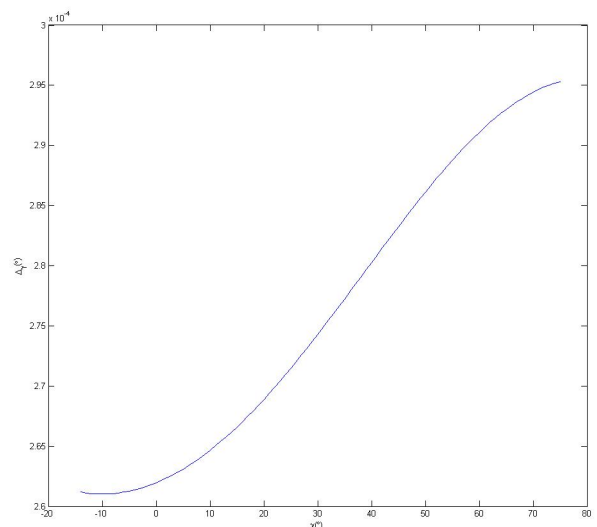


Fig. 10. A plot of the function  $\Delta_\gamma(\phi, \theta)$

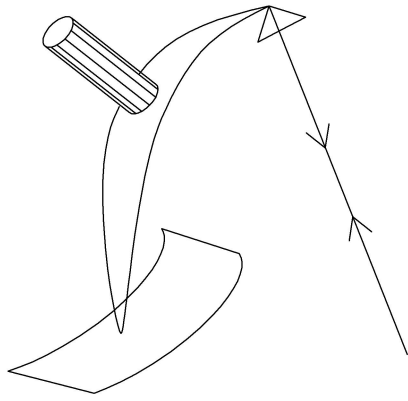


Fig. 11. Measuring hidden objects

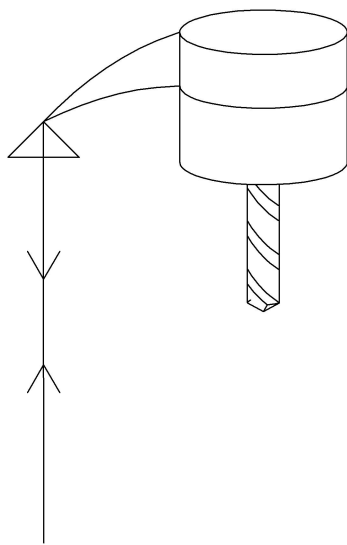


Fig. 12. Positioning

One possible application is proposed by Bridges et al. (2010). It is measuring of hidden or inaccessible surfaces. We just propose a bit more elegant device for this purpose, which is shown on Figure 11. The idea of the device is that if you know where the head of the device (cube corner) resides and a coordinate system attached to the head, then you also know where the foot of the device is placed on a hidden measured surface.

The next suggesting itself application is positioning. For example Figure 12 shows controlling the end of a rotating drill with a single cube corner. Other possible areas of this application cover various input devices like mouses, joysticks, trackers and so on. Knowing orientation adds these devices an ability to provide much more information simultaneously.

A big group of applications deals with vehicles. In these applications the coordinate system attached to a cube corner is used for controlling vehicles in the space surrounding the cube corner. High accuracy computing of this coordinate system allows a spacecraft to dock itself or join with another spacecraft by means of a single cube corner. Similar applications are possible for airplanes, see Figure 13.

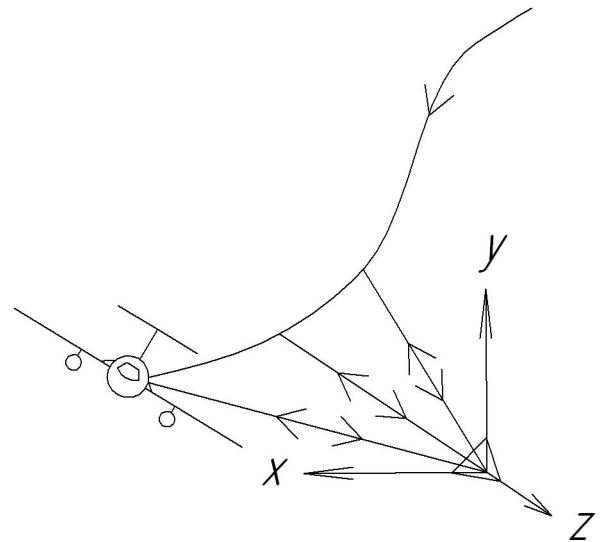


Fig. 13. Docking

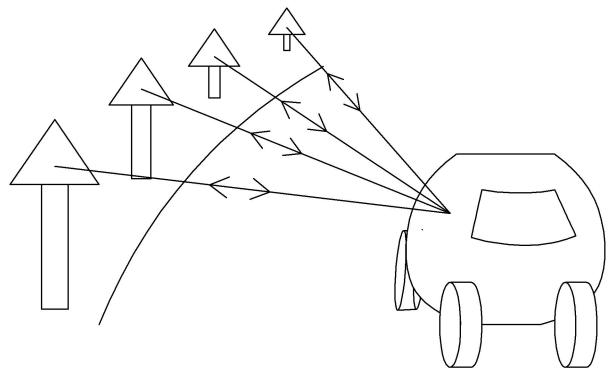


Fig. 14. Road making

Finally, recall that cube corners are, in fact, already used in road making. They are so called cat's eyes. However, cat's eyes are used only to help a human driver to see the path the vehicle follows. Knowing the orientation of the cat's eyes on the road allows a car to follow the road without a human. Really, suppose an autopilot sees one cat's eye. Hence, it knows where the wayside is.

Then one axis of the coordinate system of a cat's eye may point to the next cat's eye. The rotation of the cat's eye about this axis may code the distance to the next cat's eye. Knowing both the direction to the next cat's eye and the distance to it, the autopilot is able to find the next cat's eye and drive the vehicle toward it to repeat the same operations once again, see Figure 14.

#### REFERENCES

- Bridges, R.E., Brown, L.B., West, J.K., and Ackerson, D.S. (2010). Laser-based coordinate measuring device and laser-based method for measuring coordinates. Patent US 7,800,785 B1.
- Dukarevich, J.E. and Dukarevich, M.J. (2009). Absolute angle transducer (versions). Patent RU 2,419,067 C2.
- Matveev, M.N. (2014). A method of determining orientation with an optical system and a cube corner. Patent Application RU 2014108388.